Third Joint Eurohaptics Conference and Symposium on Haptic Interfaces
for Virtual Environment and Teleoperator Systems
Salt Lake City, UT, USA, March 18-20, 2009

Maneuverability of Master Control Devices Considering the Musculo-skeletal Model of an Operator

Sho Ito*
Department of Mechanical
Engineering and Science
Kyoto University

Yasuyoshi Yokokohji†
Department of Mechanical
Engineering and Science
Kyoto University

ABSTRACT

In this paper, maneuverability measure of master control devices considering the musculo-skeletal model of operators is proposed. The original maneuverability measure of master arms considering the operator dynamics is extended by introducing a muscle tension space instead of the joint torque space of an operator so that the maneuverability is evaluated under a constant muscle stress condition which is related to muscle fatigue. Unidirectionality of muscle tension forces as well as the gravity effects acting on the master device and the operator arm are explicitly considered to get a correct evaluation.

As a numerical example, the effect of a movable armrest installed on a master arm is evaluated based on the proposed measure. It is shown that the armrest is effective to reduce muscle fatigue by not only lowering the gravity loads for the operator but also reducing the gripping force necessary to maneuver the device. Experiments are also conducted to verify the result of this numerical example.
Keywords: maneuverability, master control device, haptic device, musculo-skeletal model, fatigue

1 INTRODUCTION

Maneuverability of control devices in human-machine interaction systems is an important factor. Typical examples of such control devices are master arms and joysticks for teleoperation systems and haptic devices for virtual reality simulation and training systems. Such control devices must be designed so that human operators can use them for a long time without getting fatigued.

Armrests are often installed to the control devices in order to reduce the fatigue of the operator. Most of armrests are fixed on the ground, which can be seen in many master control stations of surgical robots including da Vinci, but an armrest can be movable as shown in Fig.1. This master arm was developed by the authors to teleopearte a heavy-duty hydraulic dual-arm robot (T-52 Enryu), which was exhibited at the Aichi EXPO in 2003 together with T-52 Enryu [2]. The developed master arm is called "semi-exoskeleton type" taking both advantages from the conventional fixed armrest (reducing the fatigue) and the conventional exoskeleton master (wide working volume).

The developed master arm showed good performance and the operator could continue to use it for a long time without serious fatigue. Possible reasons for that are: (i) The armrest supported a part of the weight of the operator arm, and (ii) By applying forces to the master arm through the armrest, the operator could reduce the gripping force necessary for resisting the interaction force at the handgrip. Note that the first one is obvious and the second possibility is valid only for the movable armrests like the one shown in Fig.1. We also empirically know that maneuvering an exoskeleton master becomes easier when the upper arm part is strapped so that the operator can apply forces to the master not only through the handgrip but also through the elbow. In this case, the second possibility could be the reason.

In this paper, a maneuverability measure of master control devices considering the fatigue of an operator is proposed. To analyze the maneuverability of a master control device, we have to consider not only the dynamics of the master device but also the dynamics of an operator. Introducing the musculo-skeletal model of operators, the original maneuverability measure of master arms, which was previously proposed by the authors [1], is extended to evaluate the mapping from a muscle tension space to a master arm acceleration space so that fatigue of an operator can be considered. Unidirectionality of muscle tension forces as well as the gravity effects acting on the master device and the operator arm are explicitly considered to get a correct evaluation. It is shown that a set of resultant accelerations of a master arm under the constant muscle stress norm condition forms an ellipsoid and we define a maneuverability measure as the volume of this ellipsoid like the original manipulability measure. It is known that muscle stress, i.e., muscle tension divided by its physiological cross-sectional area (PCSA), determines the endurance of that muscle [3]. Therefore, muscle stress is highly related to muscle fatigue.

As a numerical example, we evaluated the effect of the movable armrest quantitatively based on the proposed measure. It is shown that the armrest is effective to reduce muscle fatigue in the way that it not only lowers the gravity loads (the first possibility mentioned above) but also reduces the gripping force to maneuver the device (the second possibility). Experiments are also conducted to verify the result of this numerical example.

2 MANEUVERABILITY FORMULATION

2.1 Dynamics of master arm and operator

In this section, the formulation by the authors [1] is extended to the case where gravity is applied and an armrest is installed on the master arm. We assume that an operator is grasping a handgrip attached to the endpoint of a master arm and resting his elbow on the armrest. As shown in Fig.2, there are two interaction points between the master device and the operator arm, an arm handgrip and an armrest, through which interaction forces are applied. We assume that the master arm behaves passively, i.e., joint actuators

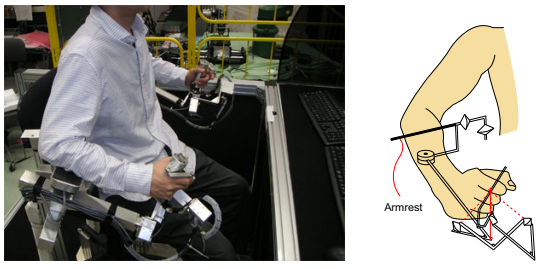

(a) Overview (b) Arm structure

Figure 1: Semi-exoskeleton dual-arm master

*e-mail: sho@blue.mbox.media.kyoto-u.ac.jp
†e-mail: yokokohji@me.kyoto-u.ac.jp

are not activated. Then we can regard the operator arm as a robot arm which carries the passive master arm as a payload.

We assume that the operator and master arms are n_{op}-DOF and n_m-DOF ($n_m \leq n_{op}$), respectively. We define the common endpoint vector of the operator and the master arms as $\boldsymbol{r} \in \Re^m$, where m ($\leq n_{op}$) is the dimension of the task space of the operator arm. Note that n_m can be either $n_m \geq m$, meaning that the master arm could be redundant, or $n_m < m$, meaning that the master arm constraints the operator's hand motion. Even if the master arm is redundant, i.e., $n_m > m$, its configuration must be deterministic, i.e., given a configuration of the operator arm in the coupled system, the configuration of the master arm must be determined uniquely due to the constraints at two interaction points.

Equations of motion of the operator and the master arm are given respectively as

$$\boldsymbol{\tau}_{op} = \boldsymbol{M}_{op}\ddot{\boldsymbol{\theta}}_{op} + \boldsymbol{g}_{op} + \boldsymbol{J}_{op1}^T \boldsymbol{f}_1 + \boldsymbol{J}_{op2}^T \boldsymbol{f}_2, \quad (1)$$

$$\boldsymbol{0} = \boldsymbol{M}_m\ddot{\boldsymbol{\theta}}_m + \boldsymbol{g}_m + \boldsymbol{J}_{m1}^T(-\boldsymbol{f}_1) + \boldsymbol{J}_{m2}^T(-\boldsymbol{f}_2), \quad (2)$$

where $\boldsymbol{\tau}_{op} \in \Re^{n_{op}}$ and $\boldsymbol{\theta}_{op} \in \Re^{n_{op}}$ denote the joint torque vector and the joint angle vector of the operator and $\boldsymbol{\theta}_m \in \Re^{n_m}$ means the joint angle (or displacement in general) of the master arm. Matrices $\boldsymbol{M}_{op} \in \Re^{n_{op} \times n_{op}}$ and $\boldsymbol{M}_m \in \Re^{n_m \times n_m}$ are the inertia matrices of the operator and the master arm, respectively. The forces that the operator applies to the master arm through the handgrip and the armrest are denoted by $\boldsymbol{f}_1 \in \Re^m$ and $\boldsymbol{f}_2 \in \Re^m$, respectively. Two matrices, $\boldsymbol{J}_{op1} \in \Re^{m \times n_{op}}$ and $\boldsymbol{J}_{op2} \in \Re^{m \times n_{op}}$, are Jacobians of the operator hand and the operator elbow, respectively. Similarly, $\boldsymbol{J}_{m1} \in \Re^{m \times n_m}$ and $\boldsymbol{J}_{m2} \in \Re^{m \times n_m}$ are defined for the master. Note that $m_{op2} \triangleq \mathrm{rank}(\boldsymbol{J}_{op2}) < m$ and $m_{m2} \triangleq \mathrm{rank}(\boldsymbol{J}_{m2}) < m$. Gravity terms are $\boldsymbol{g}_{op} \in \Re^{n_{op}}$ for the operator arm and $\boldsymbol{g}_m \in \Re^{n_m}$ for the master arm.

Since the operator holds the handgrip of the master device firmly, joint accelerations must satisfy the following constraint:

$$\boldsymbol{J}_{op}\ddot{\boldsymbol{\theta}}_{op} = \boldsymbol{J}_m\ddot{\boldsymbol{\theta}}_m, \quad (3)$$

where we neglected velocity terms.

When the operator elbow is completely constrained at the armrest of the master arm, the following constraint holds:

$$\boldsymbol{J}_{op2}\ddot{\boldsymbol{\theta}}_{op} = \boldsymbol{J}_{m2}\ddot{\boldsymbol{\theta}}_m, \quad (4)$$

where we again neglected velocity terms. To extract independent constraints from (4), a matrix $\boldsymbol{E}_2 = \begin{bmatrix} \boldsymbol{e}_{21} & \boldsymbol{e}_{22} & \cdots & \boldsymbol{e}_{2m_2} \end{bmatrix} \in \Re^{m \times m_2}$ is introduced and a set of independent constraints is given by

$$\boldsymbol{E}_2^T \boldsymbol{J}_{op2}\ddot{\boldsymbol{\theta}}_{op} = \boldsymbol{E}_2^T \boldsymbol{J}_{m2}\ddot{\boldsymbol{\theta}}_m, \quad (5)$$

where $\boldsymbol{e}_{2j}$ ($j = 1, \cdots m_2$) denotes a vector in the constraint direction and m_2 ($= \max(m_{op2}, m_{m2})$) is the number of independent constraints at the elbow. Usually each $\boldsymbol{e}_{2j}$ is chosen to be an unit vector, being orthogonal each other but not limited to such setting.

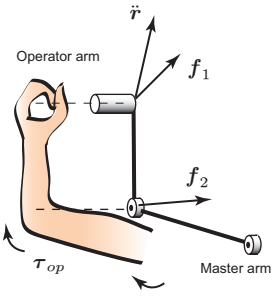

Figure 2: Operator manipulating a master arm by applying force through handgrip (hand) and armrest (elbow)

Usually under the constraint of (5), m constraints at the endpoint given by (3) are no longer independent. In fact, if $m + m_2 > n_{op}$, it is obviously over-constraint. To extract independent components from (3) under the constraint of (5), another matrix $\boldsymbol{E}_1 = \begin{bmatrix} \boldsymbol{e}_{11} & \boldsymbol{e}_{12} & \cdots & \boldsymbol{e}_{1m_1} \end{bmatrix} \in \Re^{m \times m_1}$ is introduced and a set of independent constraints is given by

$$\boldsymbol{E}_1^T \boldsymbol{J}_{op1}\ddot{\boldsymbol{\theta}}_{op} = \boldsymbol{E}_1^T \boldsymbol{J}_{m1}\ddot{\boldsymbol{\theta}}_m, \quad (6)$$

where $\boldsymbol{e}_{1j}$ ($j = 1, \cdots m_1$) denotes a vector in the constraint direction and m_1 ($\leq m$) is the number of independent constraints at the endpoint. Usually each $\boldsymbol{e}_{1j}$ is chosen to be an unit vector, being orthogonal each other but not limited to such setting. Constraints (5) and (6) are no longer over-constraint and $m_1 + m_2 \leq n_{op}$ holds. Especially when there is no elbow constraint, $m_1 = m$ and $m_2 = 0$.

Defining new vectors $\hat{\boldsymbol{f}}_1 \in \Re^{m_1}$ and $\hat{\boldsymbol{f}}_2 \in \Re^{m_2}$ each of which element denotes the component of the constraint forces along with the corresponding constraint direction, $\boldsymbol{f}_1$ and $\boldsymbol{f}_2$ are given by $\boldsymbol{f}_1 = \boldsymbol{E}_1\hat{\boldsymbol{f}}_1$ and $\boldsymbol{f}_2 = \boldsymbol{E}_2\hat{\boldsymbol{f}}_2$, respectively. Then combining (1), (2), (5), and (6) all together, we get

$$\begin{bmatrix} \boldsymbol{M} & \tilde{\boldsymbol{J}}^T \\ \tilde{\boldsymbol{J}} & \boldsymbol{0} \end{bmatrix} \begin{bmatrix} \ddot{\boldsymbol{\theta}} \\ \hat{\boldsymbol{f}} \end{bmatrix} = \begin{bmatrix} \boldsymbol{\tau} \\ \boldsymbol{0} \end{bmatrix}, \quad (7)$$

where $\boldsymbol{M}$, $\tilde{\boldsymbol{J}}$ are defined as

$$\boldsymbol{M} \triangleq \begin{bmatrix} \boldsymbol{M}_{op} & \boldsymbol{0} \\ \boldsymbol{0} & \boldsymbol{M}_m \end{bmatrix}, \ \tilde{\boldsymbol{J}} \triangleq \begin{bmatrix} \boldsymbol{E}_1^T\boldsymbol{J}_{op1} & -\boldsymbol{E}_1^T\boldsymbol{J}_{m1} \\ \boldsymbol{E}_2^T\boldsymbol{J}_{op2} & -\boldsymbol{E}_2^T\boldsymbol{J}_{m2} \end{bmatrix}, \quad (8)$$

and $\ddot{\boldsymbol{\theta}}$, $\hat{\boldsymbol{f}}$, $\boldsymbol{\tau}$ are defined as

$$\ddot{\boldsymbol{\theta}} \triangleq \begin{bmatrix} \ddot{\boldsymbol{\theta}}_{op} \\ \ddot{\boldsymbol{\theta}}_m \end{bmatrix}, \ \hat{\boldsymbol{f}} \triangleq \begin{bmatrix} \hat{\boldsymbol{f}}_1 \\ \hat{\boldsymbol{f}}_2 \end{bmatrix}, \ \boldsymbol{\tau} \triangleq \begin{bmatrix} \boldsymbol{\tau}_{op} - \boldsymbol{g}_{op} \\ -\boldsymbol{g}_m \end{bmatrix}. \quad (9)$$

From (7), one can solve $\ddot{\boldsymbol{\theta}}$ and $\hat{\boldsymbol{f}}$ from a given $\boldsymbol{\tau}$ as:

$$\begin{aligned} \ddot{\boldsymbol{\theta}} &= [\boldsymbol{M}^{-1} - \boldsymbol{M}^{-1}\tilde{\boldsymbol{J}}^T(\tilde{\boldsymbol{J}}\boldsymbol{M}^{-1}\tilde{\boldsymbol{J}}^T)^{-1}\tilde{\boldsymbol{J}}\boldsymbol{M}^{-1}]\boldsymbol{\tau} \\ &\triangleq \boldsymbol{W}\boldsymbol{\tau} = \begin{bmatrix} \boldsymbol{W}_{11} & \boldsymbol{W}_{12} \\ \boldsymbol{W}_{21} & \boldsymbol{W}_{22} \end{bmatrix} \begin{bmatrix} \boldsymbol{\tau}_{op} - \boldsymbol{g}_{op} \\ -\boldsymbol{g}_m \end{bmatrix}, \quad (10) \\ \hat{\boldsymbol{f}} &= (\tilde{\boldsymbol{J}}\boldsymbol{M}^{-1}\tilde{\boldsymbol{J}}^T)^{-1}\tilde{\boldsymbol{J}}\boldsymbol{M}^{-1}\boldsymbol{\tau} \\ &\triangleq \boldsymbol{H}\boldsymbol{\tau} = \begin{bmatrix} \boldsymbol{H}_{11} & \boldsymbol{H}_{12} \\ \boldsymbol{H}_{21} & \boldsymbol{H}_{22} \end{bmatrix} \begin{bmatrix} \boldsymbol{\tau}_{op} - \boldsymbol{g}_{op} \\ -\boldsymbol{g}_m \end{bmatrix}. \quad (11) \end{aligned}$$

Extracting $\ddot{\boldsymbol{\theta}}_m$ from (10) and transforming it to the endpoint acceleration, we get a mapping from $\boldsymbol{\tau}_{op}$ to $\ddot{\boldsymbol{r}}$ as:

$$\begin{aligned} \ddot{\boldsymbol{r}} &= \boldsymbol{J}_{m1}\ddot{\boldsymbol{\theta}}_m = \boldsymbol{J}_{m1}(\boldsymbol{W}_{21}\boldsymbol{\tau}_{op} - \boldsymbol{W}_{21}\boldsymbol{g}_{op} - \boldsymbol{W}_{22}\boldsymbol{g}_m) \\ &\triangleq \boldsymbol{J}_{m1}\boldsymbol{W}_{21}\boldsymbol{\tau}_{op} - \boldsymbol{b}_{grav}, \quad (12) \end{aligned}$$

where $\boldsymbol{b}_{grav}$ denotes an offset of the endpoint acceleration due to gravity.

The number of constraints in (5) and (6) depends on how the operator arm is constrained by the master arm. It can be shown that when $\boldsymbol{J}_{op1}$ is invertible under the constraints of (3) and (4), namely $\boldsymbol{J}_{op2}\boldsymbol{J}_{op1}^{-1}\boldsymbol{J}_{m1} = \boldsymbol{J}_{m2}$ holds, we end up with the same $\boldsymbol{W}_{21}$ in (12) regardless of $\boldsymbol{E}_1$ and $\boldsymbol{E}_2$, meaning that the same joint torque $\boldsymbol{\tau}_{op}$ yields the same endpoint acceleration no matter how the elbow is constrained. In other words, only the interaction forces $\boldsymbol{f}_1$ and $\boldsymbol{f}_2$ are altered depending on the elbow constraint condition. Note here that the more constraints at the armrest, the less constraints at the endpoint so that the norm of handgrip force $\boldsymbol{f}_1 = \boldsymbol{E}_1\hat{\boldsymbol{f}}_1$ can be smaller.

2.2 Introducing muscle tension space

In the previous subsection, we formulated a mapping from the operator joint torque space to the handgrip acceleration space. In order to consider muscle fatigue of the operator, we have to introduce a musculo-skeletal model of the operator.

We assume that arm joints of an operator are driven by k muscles and define the muscle tension vector $\boldsymbol{t}_a \in \Re^k$. Then the joint torque vector corresponding to this muscle tension vector is given by

$$\boldsymbol{\tau}_{op} = \boldsymbol{G}^T \boldsymbol{t}_a, \tag{13}$$

where $\boldsymbol{G}(\boldsymbol{\theta}_{op}) \in \Re^{k \times n_{op}}$ denotes the Jacobian that maps the joint velocity to the muscle expansion and contraction velocity [5]. Substituting (13) into (12), we get

$$\ddot{\boldsymbol{r}} - \boldsymbol{b}_{grav} = \boldsymbol{J}_{m1} \boldsymbol{W}_{21} \boldsymbol{G}^T \boldsymbol{t}_a. \tag{14}$$

Now, we introduce a normalization matrix $\boldsymbol{T}_a = \sigma_{\max} \times \mathrm{diag}(s_{a1}, s_{a2}, \cdots, s_{ak})$, where σ_{max} denotes the maximum stress of a muscle fiber and $s_{ai} (i = 1, 2, \cdots, k)$ mean the physiological cross-sectional area (PCSA) of each muscle. It is known that the maximum tension of a muscle is proportional to its PCSA. PCSA can be approximately obtained by dividing the muscle volume by its total length.

Using the normalized tension (or muscle stress), $\hat{\boldsymbol{t}}_a = \boldsymbol{T}_a^{-1} \boldsymbol{t}_a$, (14) becomes

$$\ddot{\boldsymbol{r}} - \boldsymbol{b}_{grav} = \boldsymbol{J}_{m1} \boldsymbol{W}_{21} \boldsymbol{G}^T \boldsymbol{T}_a \hat{\boldsymbol{t}}_a \triangleq \widetilde{\boldsymbol{W}}_a \hat{\boldsymbol{t}}_a, \tag{15}$$

which gives the relation between the normalized tension and the resultant handgrip acceleration. Then a set of all possible handgrip accelerations under the condition of $\|\hat{\boldsymbol{t}}_a\|^2 \leq 1$ forms an ellipsoid given by

$$\ddot{\boldsymbol{r}}^T (\widetilde{\boldsymbol{W}}_a \widetilde{\boldsymbol{W}}_a^T)^+ \ddot{\boldsymbol{r}} \leq 1 \tag{16}$$

with an offset due to the gravity, $\boldsymbol{b}_{grav}$. Like the original manipulability measure [4], we can define $w_m = \sqrt{\det \widetilde{\boldsymbol{W}}_a \widetilde{\boldsymbol{W}}_a^T}$, which is proportional to the volume of the ellipsoid given by (16), as a maneuverability measure of master arms under a constant norm of the muscle stress vector.

Crowninshield and Brand [3] minimized ℓ_3-norm of muscle stress vector to get the most enduring muscle force distributions. They also showed that minimizing ℓ_2-norm, corresponding to $\|\hat{\boldsymbol{t}}_a\|^2$, gave almost the same solutions. If the degree of fatigue is not coupled among muscles, a constant muscle fatigue condition in each muscle $|\hat{t}_{a_j}| \leq 1$ forms an k-dimensional hypercube in the muscle stress space and the resultant endpoint acceleration forms an m-dimensional polytope. Then the ellipsoid given by (16) under the condition of $\|\hat{\boldsymbol{t}}_a\|^2 \leq 1$ approximates this polytope and the proposed measure w_m can be regarded as a measure of possible handgrip accelerations by the muscle tensions under the constant muscle fatigue condition.

One can also regard the constant muscle stress norm condition as the constant muscle motor command energy condition, in other words, the constant "effort" of an operator.

2.3 Unidirectionality of muscle tensions

The constant norm condition of $\|\hat{\boldsymbol{t}}_a\|^2 \leq 1$ does not care the sign of each element of $\hat{\boldsymbol{t}}_a$. But, in reality, all muscle tensions (or muscle stress) must be non-negative, namely $\hat{t}_{ai} \geq 0 \ (i = 1, \cdots, k)$. As shown in Fig.3, under the original norm condition, the muscle stress spans inside a unit hyper sphere in k-dimensional muscle stress space. Actually the feasible muscle stresses lie only inside the section of the hyper sphere where all components are non-negative.

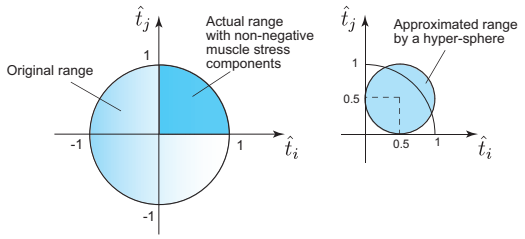

Figure 3: Approximation of input range in muscle space

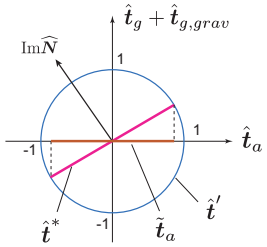

Figure 4: Feasible muscle stress (normalized tension) range

Since it is difficult to formulate a manipulability measure exactly taking the muscle stresses inside this non-negative section as inputs, we approximate this section by a hyper sphere which volume is the same as that of the exact input section as shown in Fig.3. The approximated hyper sphere has a radius of $1/2$ and its center is located at $\hat{\boldsymbol{t}}_0 = (\frac{1}{2}, \frac{1}{2}, \cdots, \frac{1}{2}) \in \Re^k$ so that all muscle stresses inside this sphere are non-negative.

Approximating the feasible muscle stress range by this hyper sphere, $\hat{\boldsymbol{t}}_a$ is given by

$$\hat{\boldsymbol{t}}_a = \frac{1}{2} \hat{\boldsymbol{t}}'_a + \hat{\boldsymbol{t}}_0, \quad \|\hat{\boldsymbol{t}}'_a\|^2 \leq 1. \tag{17}$$

Substituting (17) into (15), we get

$$\ddot{\boldsymbol{r}} - \boldsymbol{b}_{grav} - \boldsymbol{b}_0 = \widehat{\boldsymbol{W}}_a \hat{\boldsymbol{t}}'_a, \tag{18}$$

where $\boldsymbol{b}_0 = \widetilde{\boldsymbol{W}}_a \hat{\boldsymbol{t}}_0$ and $\widehat{\boldsymbol{W}}_a = \frac{1}{2} \widetilde{\boldsymbol{W}}_a$. Equation (18) means that a set of all possible accelerations forms an ellipsoid which shape is given by $\ddot{\boldsymbol{r}}^T (\widehat{\boldsymbol{W}}_a \widehat{\boldsymbol{W}}_a^T)^+ \ddot{\boldsymbol{r}} \leq 1$ and its center is offset by $\boldsymbol{b}_{grav} + \boldsymbol{b}_0$.

2.4 Gripping force

Although gripping force does not contribute to accelerating the master device, we will consider the muscles that generate gripping force as the components of the muscle tension space. We assume that these muscles generate only gripping force and do not contribute to accelerating the master devices at all. Assuming that there are l muscles generating gripping force, we can define the gripping force muscle vector as $\boldsymbol{t}_g \in \Re^l$. Combining $\boldsymbol{t}_g$ with the muscle tension vector defined in Subsection 2.2, we define the total muscle tension vector as $\boldsymbol{t} = \begin{bmatrix} \boldsymbol{t}_a^T & \boldsymbol{t}_g^T \end{bmatrix}^T \in \Re^{(k+l)}$. Introducing a new normalization matrix $\boldsymbol{T} = \sigma_{\max} \times \mathrm{diag}(s_{a1}, \cdots, s_{ak}, s_{g1}, \cdots, s_{gl}) \in \Re^{(k+l) \times (k+l)}$, where s_{gj} $(j = 1, \cdots, l)$ denotes the PCSA of the j-th gripping force muscle, the total muscle tension vector is normalized as $\hat{\boldsymbol{t}} = \boldsymbol{T}^{-1} \boldsymbol{t}$. Then we can define a new mapping from $\hat{\boldsymbol{t}}$ to $\ddot{\boldsymbol{r}}$ under the constraint of $\|\hat{\boldsymbol{t}}\|^2 \leq 1$ as a maneuverability measure of master devices under the constant muscle fatigue (or constant "effort") condition including gripping force muscles.

The larger the handgrip force is, the larger gripping force is necessary to resist it. It would be possible to obtain the exact gripping muscle tensions that balance with a given handgrip force $\boldsymbol{f}_1$ by introducing a Jacobian which specifies a mapping from muscle velocity to the velocity of the application point of $\boldsymbol{f}_1$. In practice, however, it would be difficult to derive an exact formulation

because of the indeterminateness of antagonistic muscle tensions, unidirectionality of muscle tensions, and alteration of application point depending on the direction of the handgrip force. Then, the following approximated relation is introduced:

$$\boldsymbol{t}_g = \boldsymbol{K}\left(\boldsymbol{\theta}_{op}\right)\boldsymbol{f}_1, \tag{19}$$

where $\boldsymbol{K}\left(\boldsymbol{\theta}_{op}\right) \in \Re^{l\times m}$ is a matrix specifying the gripping force muscle. The components of $\boldsymbol{t}_g$ given by (19) could be negative. In such a case, we regard that the antagonizing muscle is being activated.

From (11), $\boldsymbol{f}_1$ is given by

$$\begin{aligned}\boldsymbol{f}_1 &= \boldsymbol{E}_1\hat{\boldsymbol{f}}_1 = \boldsymbol{E}_1(\boldsymbol{H}_{11}\boldsymbol{\tau}_{op} - \boldsymbol{H}_{11}\boldsymbol{g}_{op} - \boldsymbol{H}_{12}\boldsymbol{g}_m)\\ &\triangleq \widetilde{\boldsymbol{H}}_1\boldsymbol{\tau}_{op} - \boldsymbol{h}_{grav}.\end{aligned} \tag{20}$$

Substituting (20) into (19) and considering (13), we get

$$\boldsymbol{t}_g = \boldsymbol{K}\widetilde{\boldsymbol{H}}_1\boldsymbol{G}^T\boldsymbol{t}_a - \boldsymbol{K}\boldsymbol{h}_{grav} \triangleq \boldsymbol{\Gamma}_g\boldsymbol{t}_a - \boldsymbol{t}_{grav}. \tag{21}$$

From (21), we have the following equation:

$$\begin{aligned}\boldsymbol{0} = \boldsymbol{\Gamma}_g\boldsymbol{t}_a - \boldsymbol{t}_g - \boldsymbol{t}_{grav} &= \begin{bmatrix}\boldsymbol{\Gamma}_g & -\boldsymbol{I}_l\end{bmatrix}\begin{bmatrix}\boldsymbol{t}_a\\ \boldsymbol{t}_g + \boldsymbol{t}_{grav}\end{bmatrix}\\ \triangleq \begin{bmatrix}\boldsymbol{\Gamma}_g & -\boldsymbol{I}_l\end{bmatrix}\boldsymbol{t}' &\triangleq \begin{bmatrix}\boldsymbol{\Gamma}_g & -\boldsymbol{I}_l\end{bmatrix}\boldsymbol{T}\hat{\boldsymbol{t}}' \triangleq \widehat{\boldsymbol{N}}\hat{\boldsymbol{t}}'\end{aligned} \tag{22}$$

which specifies a constraint of $\boldsymbol{t}$ when we assume the gripping force muscle tensions given by (19). A general solution of (22) is given by

$$\hat{\boldsymbol{t}}^* = (\boldsymbol{I}_{k+l} - \widehat{\boldsymbol{N}}^+\widehat{\boldsymbol{N}})\hat{\boldsymbol{t}}'. \tag{23}$$

Fig.4 conceptually illustrates this constraint in a simple 2-D space, where the original unit hypersphere $\hat{\boldsymbol{t}}'$ is projected onto the null space of $\widehat{\boldsymbol{N}}$, resulting in $\hat{\boldsymbol{t}}^*$.

Under this constraint, the muscle stress vector $\tilde{\boldsymbol{t}}_a$ is given by

$$\tilde{\boldsymbol{t}}_a = \begin{bmatrix}\boldsymbol{I}_k & \boldsymbol{O}\end{bmatrix}\hat{\boldsymbol{t}}^* = \begin{bmatrix}\boldsymbol{I}_k & \boldsymbol{O}\end{bmatrix}(\boldsymbol{I}_{k+l} - \widehat{\boldsymbol{N}}^+\widehat{\boldsymbol{N}})\hat{\boldsymbol{t}}' \triangleq \boldsymbol{Q}\hat{\boldsymbol{t}}'. \tag{24}$$

In Fig.4, $\tilde{\boldsymbol{t}}_a$ is shown as the projection of $\hat{\boldsymbol{t}}^*$ onto $\hat{\boldsymbol{t}}_a$ component. Note that $\tilde{\boldsymbol{t}}_a$ no longer spans full range of ± 1 because of the existence of the gripping force muscle tensions.

Substituting (24) into (18), we get

$$\begin{aligned}\ddot{\boldsymbol{r}} - \boldsymbol{b}_{grav} - \boldsymbol{b}_0 &= \widetilde{\boldsymbol{W}}_a\boldsymbol{Q}\hat{\boldsymbol{t}}' = \widetilde{\boldsymbol{W}}_a\boldsymbol{Q}\hat{\boldsymbol{t}} + \widetilde{\boldsymbol{W}}_a\boldsymbol{Q}\begin{bmatrix}\boldsymbol{0}\\ \boldsymbol{t}_{grav}\end{bmatrix}\\ &\triangleq \widetilde{\boldsymbol{W}}_{ag}\hat{\boldsymbol{t}} + \boldsymbol{d}_{grav}.\end{aligned} \tag{25}$$

Equation (25) means that a set of all possible handgrip accelerations under the condition of $\|\hat{\boldsymbol{t}}\|^2 \leq 1$ forms an ellipsoid which shape is specified by $\ddot{\boldsymbol{r}}^T(\widetilde{\boldsymbol{W}}_{ag}\widetilde{\boldsymbol{W}}_{ag}^T)^+\ddot{\boldsymbol{r}} \leq 1$ and its center is offset by $\boldsymbol{b}_{grav} + \boldsymbol{b}_0 - \boldsymbol{d}_{grav}$, just like (18). A new offset $\boldsymbol{d}_{grav}$ is due to the gripping force to resist the handgrip force which is necessary to hold the master device under gravity.

3 Numerical Example

In this section, we show some numerical examples based on the given formulations. As shown in Fig.5, the operator arm is modeled by a 3-DOF arm and a 2-DOF master arm which moves in a horizontal plane is considered. Making the link lengths identical to those of the corresponding links of the operator arm and locating the first joint just beneath the shoulder joint (first joint) of the operator, this master arm becomes an exoskeleton-type. Then the operator elbow is always on top of the second joint of the master arm, where we can install an armrest.

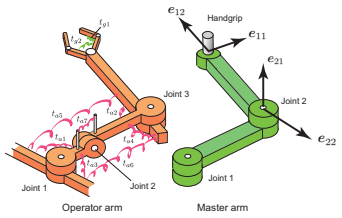

Figure 5: Musculo-skeletal model of operator arm

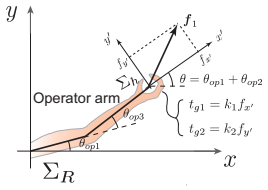

Figure 6: Handgrip force and corresponding gripping force muscle tensions

Table 1: Parameters of operator and master arm model

	operator			master	
	link1	link2	link3	link1	link2
l_i(m)	0	0.25	0.30	0.25	0.30
l_{gi} (m)	–	0.162	0.182	0.195	0.175
m_i(kg)	–	1.59	1.44	6.0	3.0
I_i(kgm^2)	–	0.0158	0.0162	0.063	0.037

Since the operator hand motion is constrained in the horizontal plane of the master arm, it is essentially 2-DOF arm driven by two pairs of mono-articular muscles and one pair of bi-articular muscles. Note, however, that the second joint must be active to balance the gravity force applying vertically when the master arm has no armrest.

Fig.5 also shows the candidates of constraint direction vectors, $\boldsymbol{e}_{1j}$ and $\boldsymbol{e}_{2j}$. Since $n_{op} = 3, m_1 + m_2 = 3$ must hold. We assume that the dimension of the gripping force muscle tension vector is two and the magnitude of each component is proportional to the projection of the handgrip force $\boldsymbol{f}_1$ onto the longitudinal and lateral directions of the forearm as shown in Fig.6. Then matrix $\boldsymbol{K}$ in (19) is given by

$$\boldsymbol{K}\left(\boldsymbol{\theta}\right) = \begin{bmatrix}k_1 & 0\\ 0 & k_2\end{bmatrix}\begin{bmatrix}\cos\theta & \sin\theta\\ -\sin\theta & \cos\theta\end{bmatrix}, \tag{26}$$

where $\theta = \theta_{op_1} + \theta_{op_3}(= \theta_{m_1} + \theta_{m_2})$. We set gains k_1 and k_2 as $k_1 = k_2 = 1.7$ based on the actual measurement of electromyogram. Gains k_1 and k_2 are related to moment-arms of the corresponding musculo-skeleton model and do not change significantly among the subjects.

Under the above mentioned setting, we consider the following four cases:

Case NA (No armrest): No armrest and no consideration of gripping forces, where $\tilde{\boldsymbol{J}} = \begin{bmatrix}\boldsymbol{J}_{op1} & -\boldsymbol{J}_{m1}\end{bmatrix}$;

Case A (Armrest but no grip force): An armrest is installed but gripping forces are not considered where $\tilde{\boldsymbol{J}}$ given by (8) is used with $\boldsymbol{E}_1 = [\boldsymbol{e}_{11}], \boldsymbol{E}_2 = \begin{bmatrix}\boldsymbol{e}_{21} & \boldsymbol{e}_{22}\end{bmatrix}$;

Case AG (Armrest and grip force): An armrest is installed and gripping forces are considered, where $\tilde{\boldsymbol{J}}$ given by (8) is used with $\boldsymbol{E}_1 = [\boldsymbol{e}_{11}], \boldsymbol{E}_2 = \begin{bmatrix}\boldsymbol{e}_{21} & \boldsymbol{e}_{22}\end{bmatrix}$;

Case FAG (Floating armrest and grip force): A "floating"-type armrest, where only vertical forces can be applied, is installed and gripping forces are considered, where $\tilde{\boldsymbol{J}}$ given by (8) is used with $\boldsymbol{E}_1 = \begin{bmatrix}\boldsymbol{e}_{11} & \boldsymbol{e}_{12}\end{bmatrix}, \boldsymbol{E}_2 = [\boldsymbol{e}_{21}]$.

Comparing Cases NA and A, we will see the effect of weight support by the armrest. Then comparing Cases A, AG and FAG, we will see the effect of introducing gripping forces and its magnitude.

We plot maneuverability ellipsoids in these four cases. To plot the ellipsoids, (18) is used for Cases NA and A and (25) is used for Cases AG and FAG.

Tables 1 and 2 summarize the parameters of the master arm and the operator arm. In Table 2, d_i means the moment arm of i-th muscle which is approximated by a constant value. The maximum muscle stress is set to $\sigma_{max} = 4.5 \times 10^5$[N/m^2]. These parameters are chosen by consulting [5][6][7].

Table 2: Muscle parameters of operator arm model

muscle #	a_1	a_2	a_3	a_4	a_5	a_6	a_7	g_1	g_2
d_i[m]	0.04	0.03	0.035	0.04	0.04	0.04	0.04	–	–
S_{ai}, S_{gi} $\times 10^{-4}$[m^2]	21.4	9.0	19.1	9.0	7.6	5.7	16.7	5.1	3.8

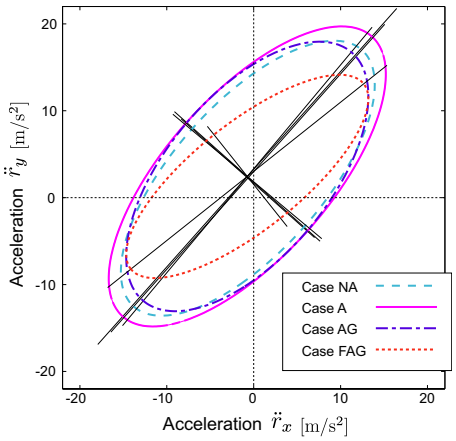

Figure 7: Dynamic manipulability ellipsoids

Fig.7 illustrates the maneuverability ellipsoids when the hand is located at $(x, y) = (0, 0.45)$[m] with respect to the base coordinate frame shown in Fig.6. Note that all ellipsoids are offset due to the unidirectionality of muscle tensions discussed in Section 2.3. Case NA gives a smaller ellipsoid than that of Case A because the operator have to activate the muscle in order to resist the gravity force when no armrest is installed. The ellipsoids in Cases AG and FAG are smaller than that of Case A because the gripping force muscles are included in these two cases. Besides, the ellipsoid in Case AG is larger than that of Case FAG because the gripping force muscle tensions become smaller and more muscle tensions can be applied for accelerating the master arm in Case AG.

4 EXPERIMENT

4.1 Experimental apparatus

We conducted an experiment to see how the muscle activities would actually change when an operator maneuver a master device with and without an armrest. Muscle activities were measured by electromyography (EMG).

We used a 3-DOF SCARA-type direct drive arm as shown in Fig.8, which was designed as an exoskeleton master arm. Since the third joint simply rotates the handgrip, this master arm is essentially the same as the one used in the numerical example. All motor powers are turned off to make the joints passive.

(a) Floating type

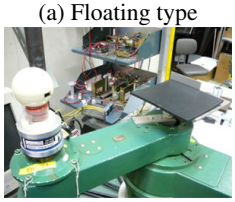

(b) Normal type

Figure 8: Two types of armrest

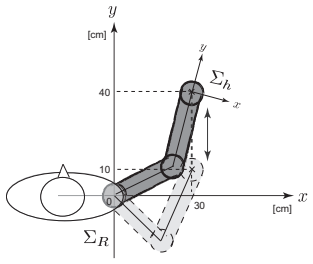

Figure 9: Arm trajectory

Two types of armrest, floating type and normal type, were prepared as shown in Fig.8. The floating type armrest has casters and moves freely in the horizontal directions and the operator cannot apply forces to the master except in the vertical direction, which corresponds to Case FAG. The normal type armrest has a free joint around the vertical axis (the second joint axis of the master) so that the operator can apply translational forces (but no moments) not only in the vertical direction but also in the horizontal direction to the master through this armrest, corresponding to Cases A and AG. Besides the two armrest cases, we also measured EMG when no armrest is installed, corresponding to Case NA. Handgrip force was measured by a 6-axis force/torque sensor mounted beneath the handgrip of the master arm.

EMGs were measured from the following four points: (EMG-a) second dorsal interossei, (EMG-b) biceps brachii, (EMG-c) deltoid, (EMG-d) greater pectoral muscle. Second dorsal interossei (EMG-a) is activated when flexing MP joint of middle finger, which is an example of the gripping force muscles. Biceps brachii (EMG-b) is activated when flexing elbow joint. Deltoid (EMG-c) is activated when abducting or extending shoulder joint. Finally, greater pectoral muscle (EMG-d) is activated when adducting or flexing shoulder joint.

A male subject (aged 23) was asked to maneuver the master arm with three different conditions, no armrest, floating-type armrest, and normal-type armrest, following a straight line back and forth as shown in Fig.9. He had to repeat the following sequence several times: move the arm forward in 1.5[s], stay at the endpoint for 2[s], move backward in 1.5[s], and stay at the other endpoint for 2[s]. A metronome was used to notify the timing of movement to the subject.

4.2 Experimental result

Fig.10 shows the experimental results. From the top, hand position $\boldsymbol{r}$, handgrip force $\boldsymbol{f}_1$, EMG-a&b, and EMG-d&e are shown in each case. Note that each EMG was plotted by an averaged rectified value (ARV) normalized by the value at the maximal voluntary contraction (MVC). Coordinates of the hand position are given with respect to the base frame shown in Fig.9. Two components of the handgrip force are given with respect to the hand frame shown in Fig.9.

Hand position profiles are almost identical in all three cases and we can assume that the operator maneuvered the master arm in the same way in all cases. When the armrest was not installed, EMG-a (second dorsal interossei) became larger when the hand was at the front end-point of the trajectory and when the hand was at the rear end-point, not only EMG-a but also EMG-c (deltoid) became larger, compared to other two cases. These muscles were activated more than other two cases in order to support the gravity force acting on the operator arm.

When the operator moved his arm backward with the original-type armrest, EMG-a (second dorsal interossei) became smaller than that with the floating-type armrest. We can also confirm the effect of the normal-type armrest from the handgrip force data. These results show that the operator could actually reduce the gripping force by applying the elbow force through the normal-type armrest.

Note that EMG-b,c,d were almost the same among the two armrest cases. This fact supports our analysis at the end of Section 2.1, i.e., as long as the operator's arm motion is deterministic for a given task, the same operator joint torque results in the same acceleration no matter how the elbow is constrained.

The proposed measure evaluates the easiness of accelerating the device at a specific configuration while in the experiment the device was moved back and forth along with a straight line, which makes the correspondence analysis difficult. From Fig.10, one can see that

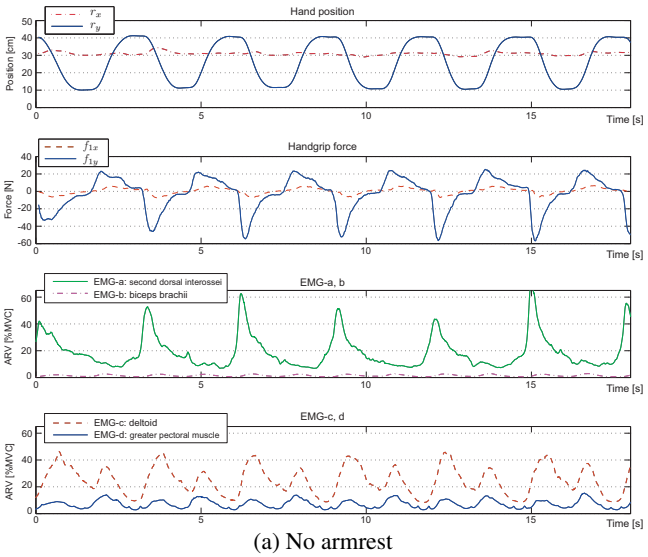

(a) No armrest

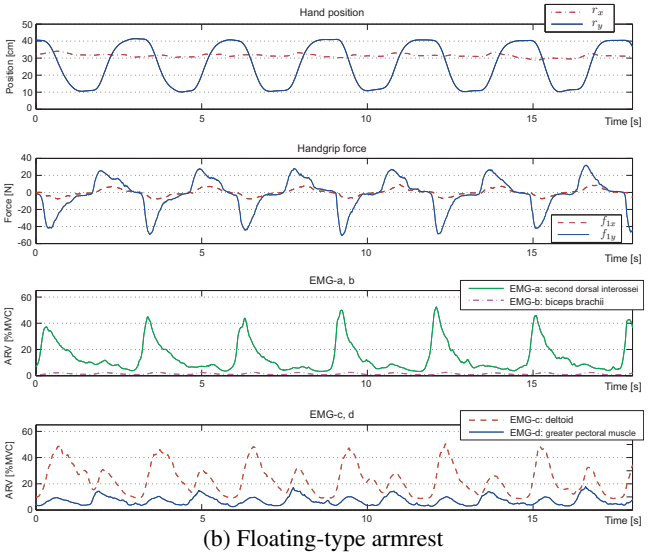

(b) Floating-type armrest

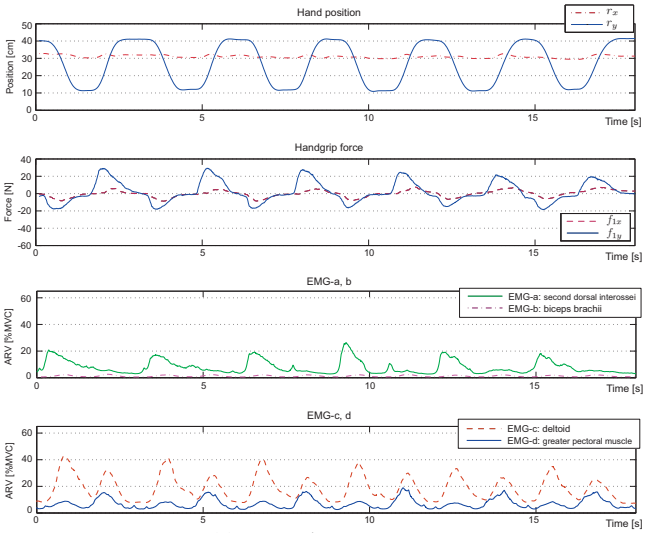

(c) Normal-type armrest

Figure 10: Experimental results

handgrip force and EMGs become large when the device is accelerated or decelerated, suggesting that the proposed measure can be applied to these points where the inertial load become dominant.

As the future works, more experiments should be conducted by using other subjects and quantitative analysis of the obtained results including the confirmation of the relevance to the actual fatigue of the subject. It is known that when a muscle fatigues the frequency shift (towards the lower frequency) of the power density spectrum of the EMG signal occurs and we can monitor this shift by observing the mean or median frequency of the EMG signal [8].

5 Conclusion

In this paper, we extended the maneuverability measure of master control devices previously proposed by the author [1] by introducing the musculo-skeletal model of operators and proposed a new maneuverability measure considering the fatigue of an operator. We formulated the mapping from a muscle tension space to a master arm acceleration space so that a set of all possible accelerations under the constant muscle stress norm condition forms an ellipsoid. Unidirectionality of muscle tension forces as well as the gravity effects were explicitly considered to get a correct evaluation.

Muscle endurance time is roughly related to the square of its stress, i.e., its tension divided by its PCSA. Then the maneuverability ellipsoid plotted under the constant muscle stress norm condition approximates the possible handgrip accelerations under the constant muscle fatigue condition. One can also regard the constant muscle stress norm condition as the constant muscle motor command energy condition, in other words, the constant "effort" of an operator. In this sense, the larger maneuverability a master device has, the less fatigue is induced to do the same manipulation task.

As a numerical example, we evaluated the effect of the movable armrest quantitatively based on the proposed measure. It was shown that the armrest is effective to reduce muscle fatigue in the way that it not only lowers the gravity loads for the operator but also reduces the gripping force when maneuvering the device. Experiments were also conducted to verify the result of this numerical example.

The proposed measure is useful for evaluating the maneuverability of master control devices for teleoperation and haptic devices for virtual reality.

References

[1] Y. Yokokohji and T. Yoshikawa, "Design Guide of Master Arms Considering Operator Dynamics," ASME Journal of Dynamic Systems, Measurement and Control, Vol.115, No.2(A), pp. 253-260, 1993.

[2] Y. Sato, K. Kawata, K. Shiratsuchi, Y. Yokokohji, and tmsuk co.,Ltd, "Development of Semi-exoskeleton Master Arms to Teleoperate a Heavy-duty Dual-arm Robot for Rescue Assistance," Proc. 36th International Symposium on Robotics (ISR 2005), November 29-December 1, Tokyo, Japan, CD-ROM, 2005.

[3] R. D. Crowninshield and R. A. Brand: "A Physiologically Based Criterion of Muscle Force Prediction in Locomotion," Journal of Biomechanics, Vol.14, No.11, pp793–801, 1981.

[4] T. Yoshikawa, "Foundations of Robotics," The MIT Press, 1990.

[5] T. Tsuji, K. Ito, M. Nagamachi, and T. Ikemoto, "Impedance Regulations in Musculo-Motor Control System and the Manipulation Ability of the End-Point," Trans. of Society of Instrument and Control Engineers, Vol.24, No.4, pp.385–392, 1988. (*in Japanese*)

[6] K. R. S. Holzbaur *et al.*, "A Model of the Upper Extremity for Simulating Musculoskeletal Surgery and Analyzing Neuromuscular Control," Annals of Biomedical Engineering, Vol.33, No.6, pp.829–840, 2005.

[7] I. A. Kapandji, "The Physiology of the Joints, Vol.1 Upper Limb", Churchill Livingstone, 1982.

[8] J. V. Basmajian and C. J. De Luca, "Muscles Alive: Their Functions Revealed by Electromyography (5th Ed.)", Williams & Wilkins, 1985.